ISOLDE: laser ion source

Nuclear shape coexistence via α- and β-decay studies with the application of the laser ion source

А. Е. Барзах, П. Л. Молканов,
М. Д. Селиверстов, Д. В. Федоров

Windmill-ISOLTRAP-RILIS collaboration

PNPI, Gatchina, Russian Federation

RILIS and ISOLDE, Geneva, Switzerland

Institut für Physik, Johannes Gutenberg-Universität Mainz, Mainz, Germany

University of Manchester, UK

MR-TOF@ISOLTRAP team

University of the West of Scotland, United Kingdom

Instituut voor Kern- en Stralingsfysica, K.U. Leuven, Leuven, Belgium

Comenius University, Bratislava, Slovakia

University of York, United Kingdom

… … …

IS 456, 466, 511, 534, 598, 608

α- and β-decay studies at Windmill

Windmill station

Main information:

I, $\delta\langle r^2\rangle$, μ, Q

Additional information:

$T_{1/2}$
E_α, b_α, b_β
Q_α (masses)
α-γ, γ -γ coincidence
levels, E_γ
hindrance factors
transition multipolarities
conversion coefficients
E0 transitions
partial decay schemes
(isomer selectivity)

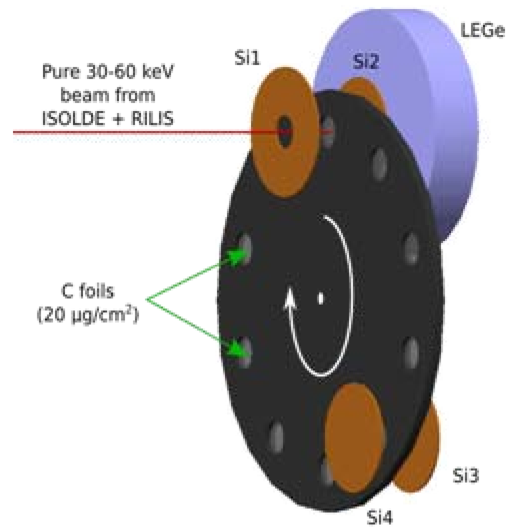

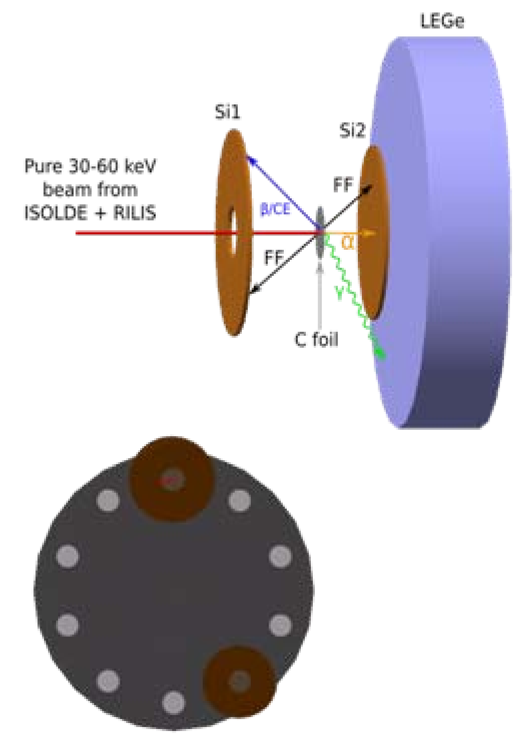

Isomer selective α and β decays

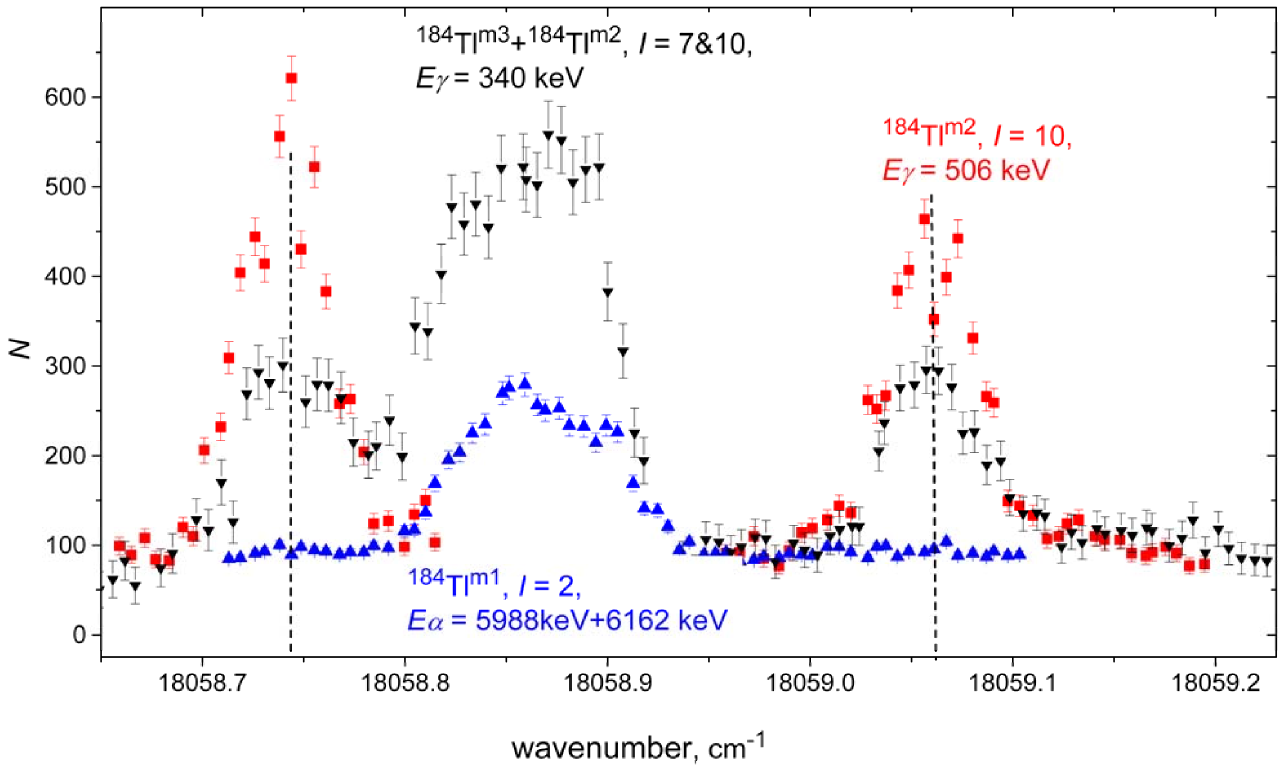

Isomer selective α and β decays

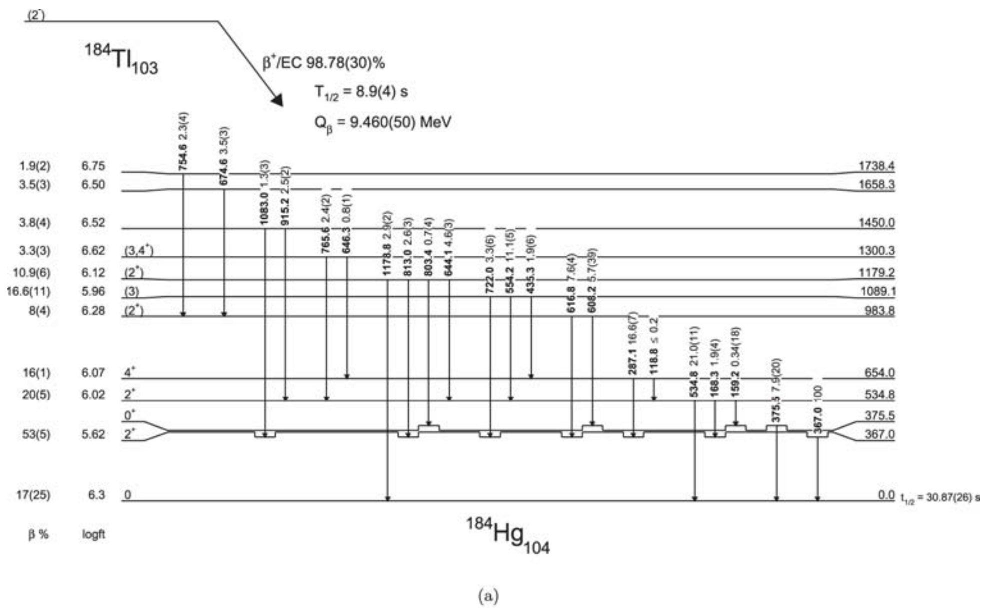

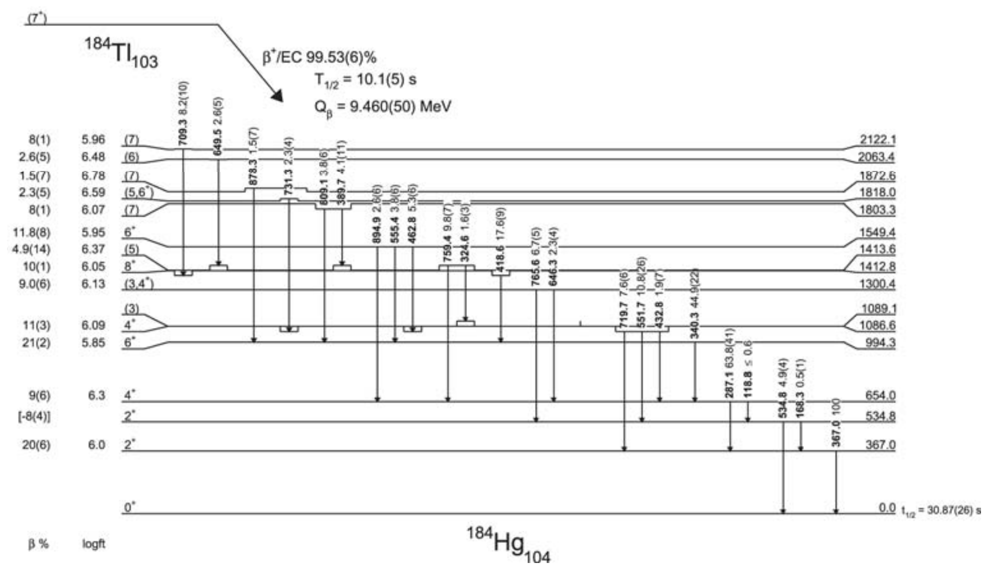

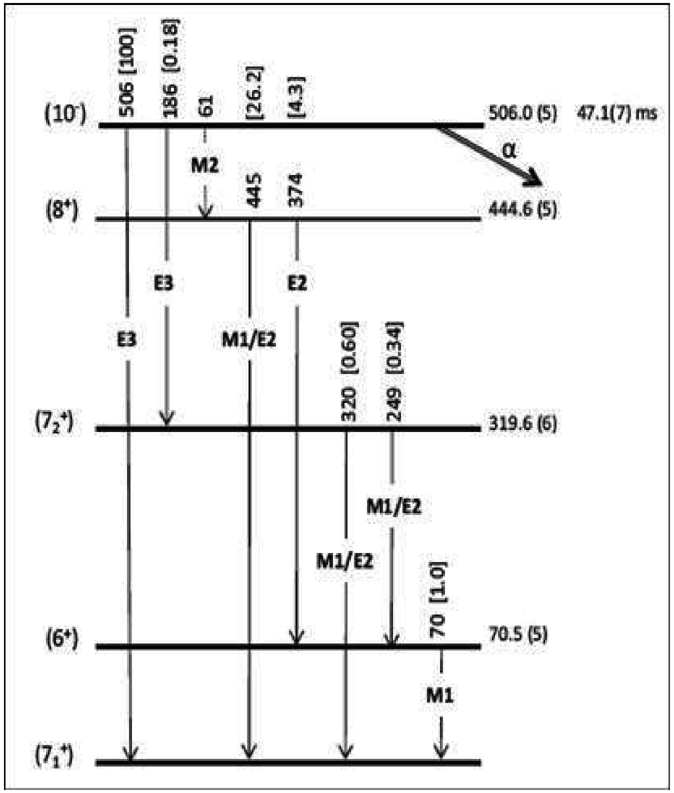

IT decay of $^{184}Tl^{m}$ (I = 10)

Hindered α decay $^{181}Tl \rightarrow {}^{177}Au$

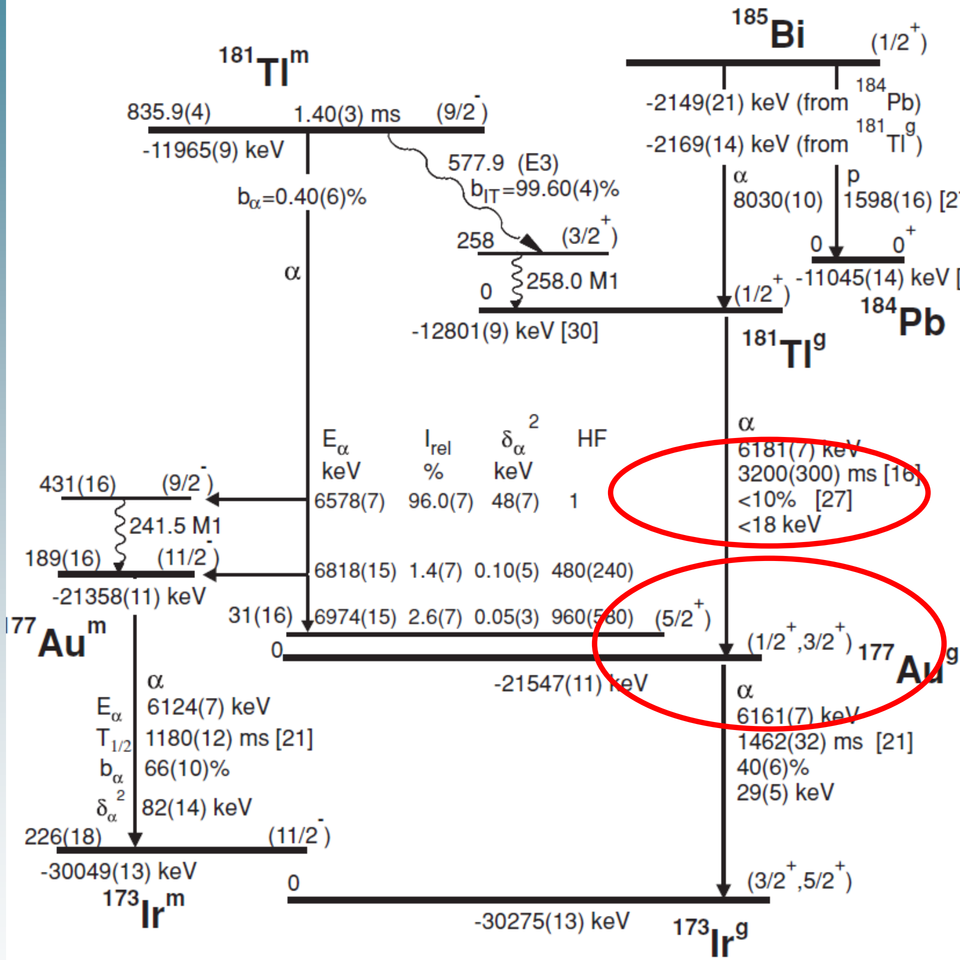

$$\delta_\alpha^2 = \frac{b_\alpha \ln(2)}{T_{1/2}} \frac{h}{P},$$

$$P = \exp\left[-2\int_{R_i}^{R_o} \frac{2\mu^{1/2}}{h}\left(V - Q_\alpha\right)^{1/2} dr\right]$$

Why is α decay of $1/2^+$ gs of ^{181}Tl hindered, HF>3?
Different spins: ^{181}Tl ($1/2^+$) and ^{177}Au ($3/2^+$)?

Spins of $^{177,\,179}$Au

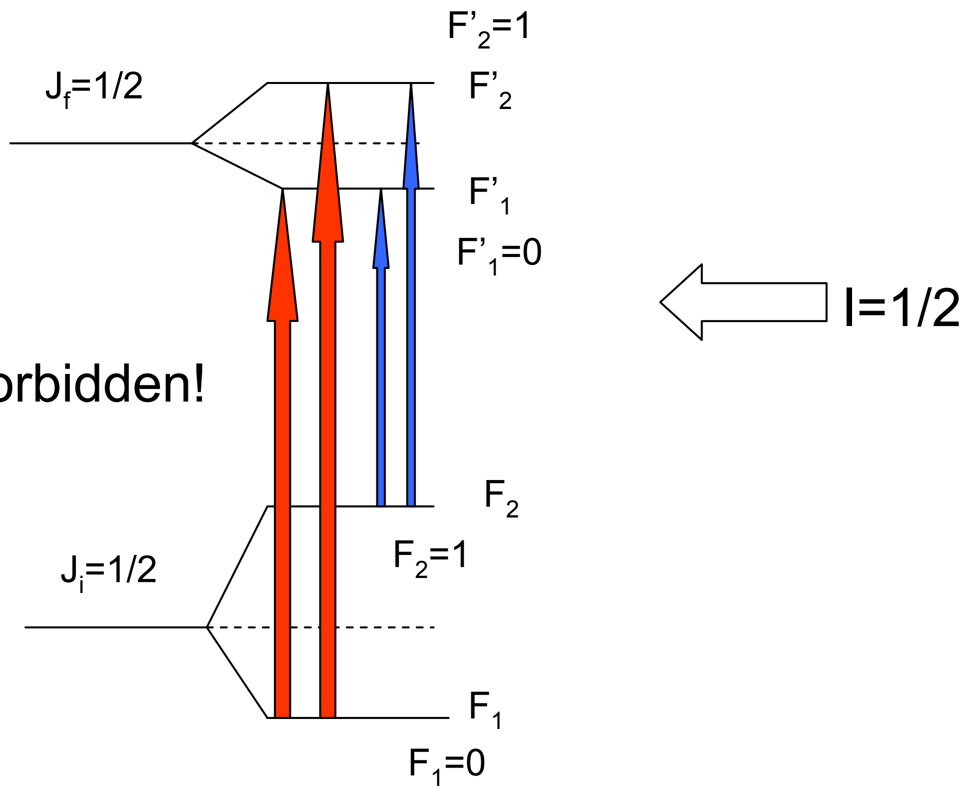

0—>0 transition is forbidden!

Only 3 rather than usual 4 lines will be seen in the hfs spectra of isotopes with I=1/2

Spins of ^{177,179}Au

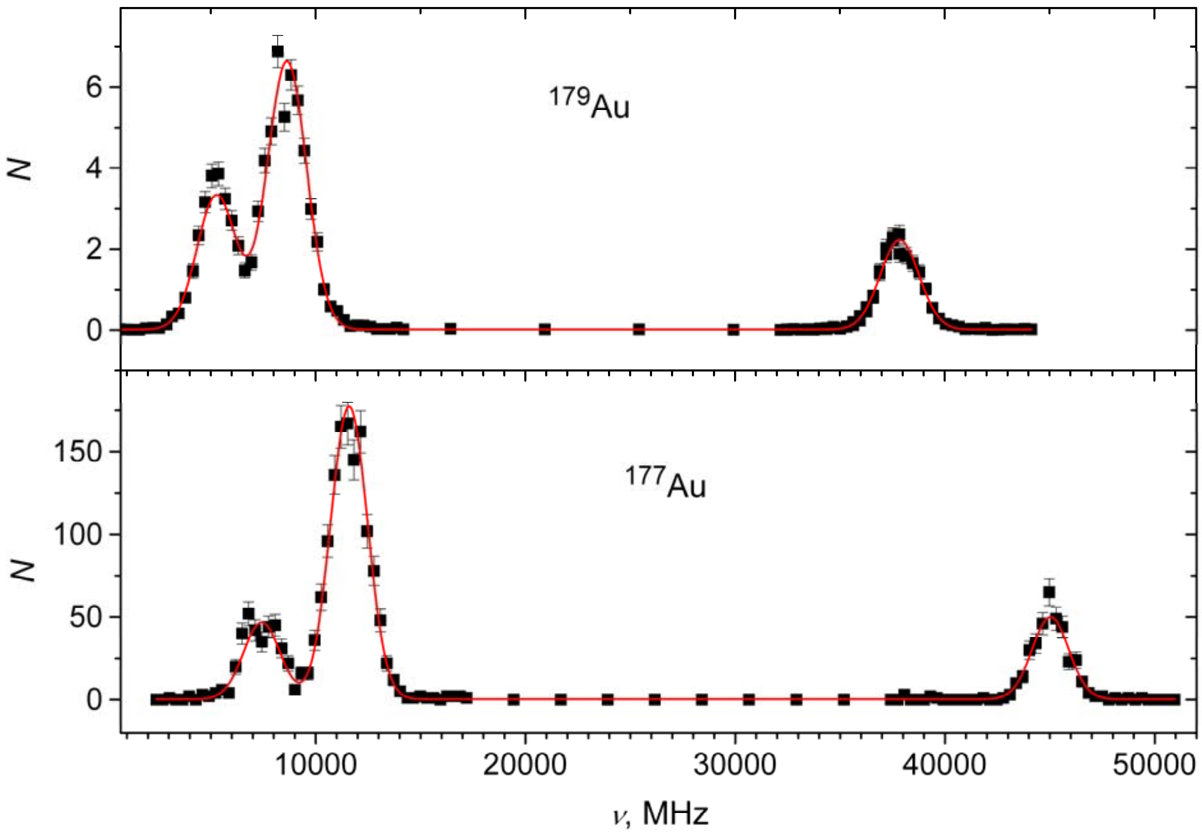

$I(^{177,179}Au) = 1/2$

Hindrance factors and μ

reduced width for $1/2^+ \rightarrow 1/2^+$ α decay

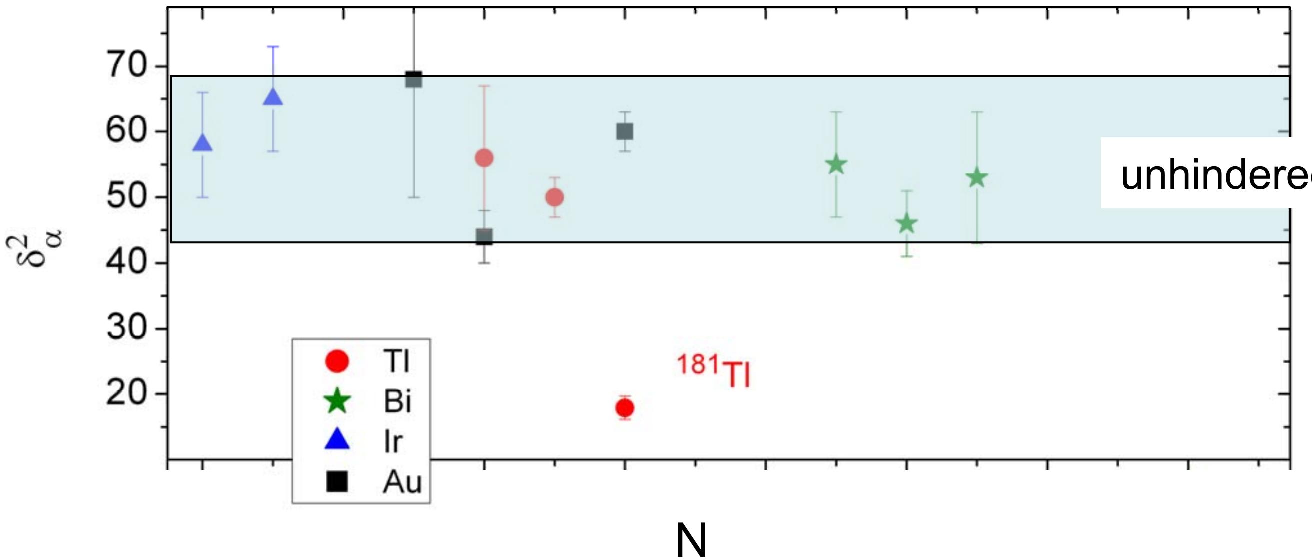

unhindered $1/2^+ \rightarrow 1/2^+$ decay

Nonaxiality in $^{177,\,179}$Au

$^{177,\,179}$Au, μ ~ 1n.m.

$^{187,\,189}$Au, μ ~ 0.5n.m.

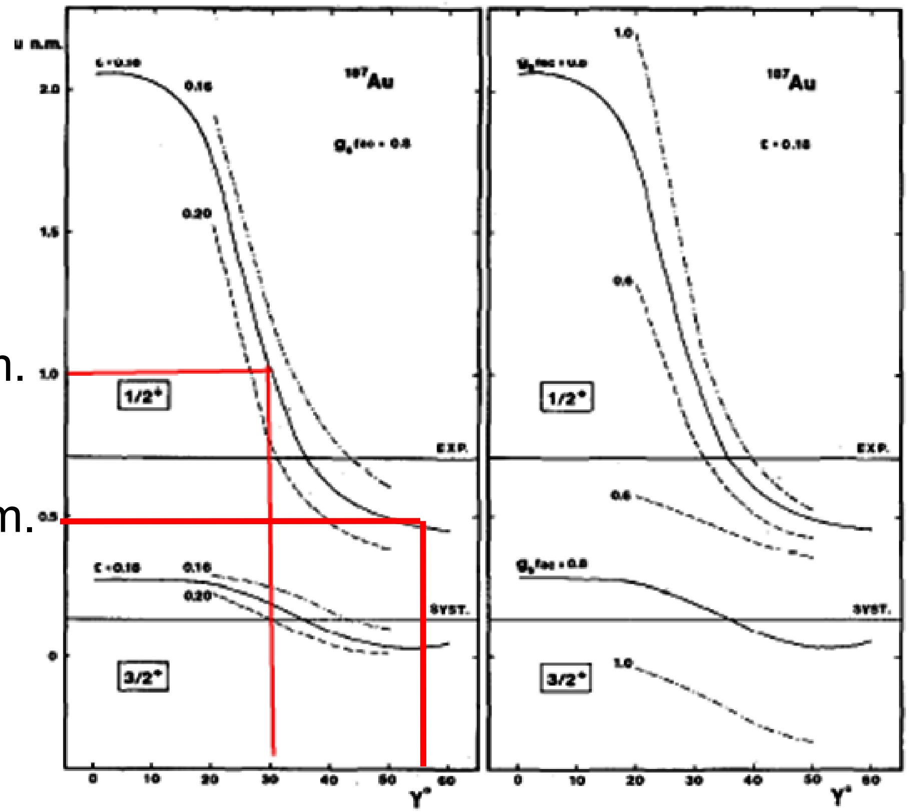

Thus, the structures of $1/2^+$ states in parent ^{181}Tl and daughter ^{177}Au are different: spherical $s_{1/2}$ state in ^{181}Tl and nonaxially deformed mixture of $s_{1/2}$ and $d_{3/2}$ states in ^{177}Au → hindrance of the α decay

Potential energy surface calculations

^{177}Au

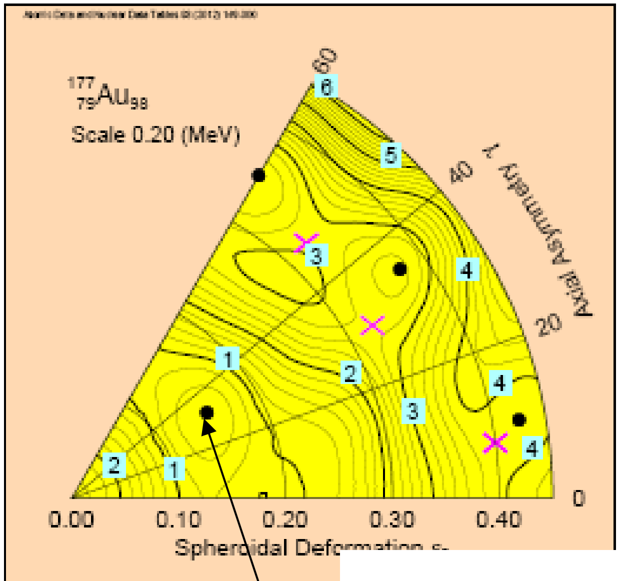

^{187}Au

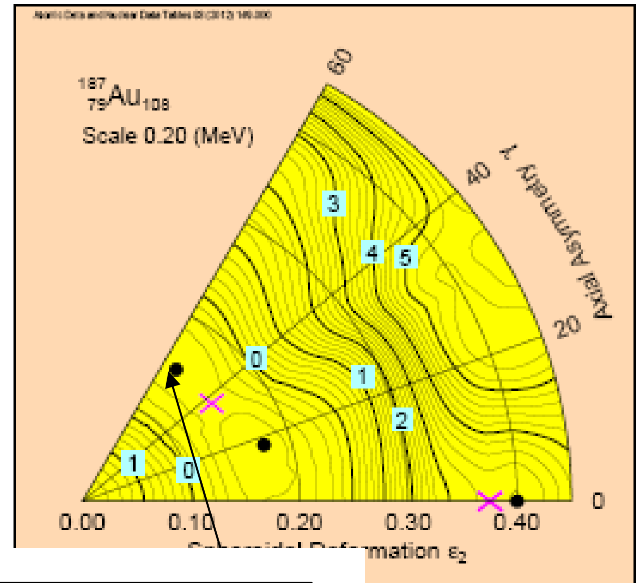

β ~ 0.17, γ ~ 30

0° (oblate)

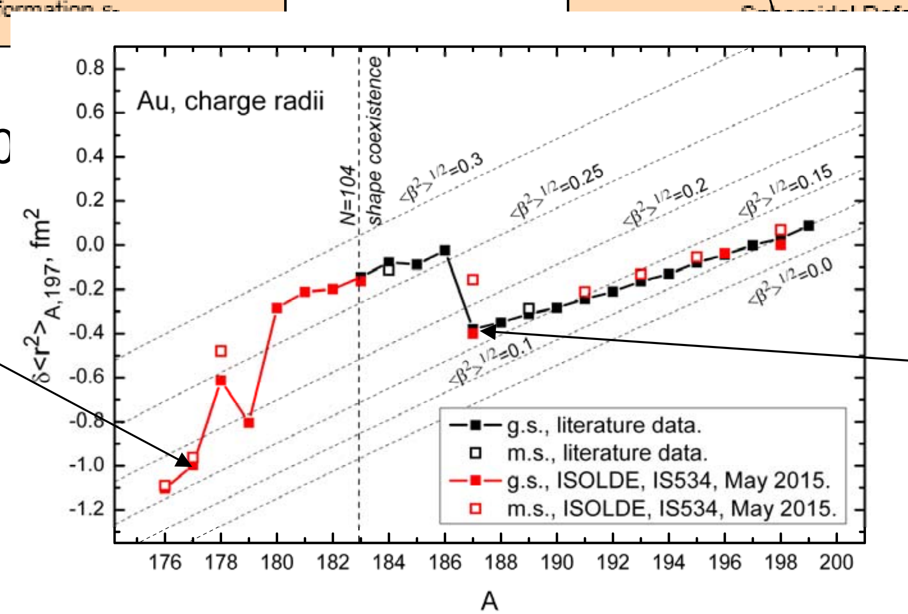

^{177}Au

$<\beta^2>^{1/2} \sim 0.17$

^{187}Au

$<\beta^2>^{1/2} \sim 0.17$

Unhindered α decay of ^{179}Tl

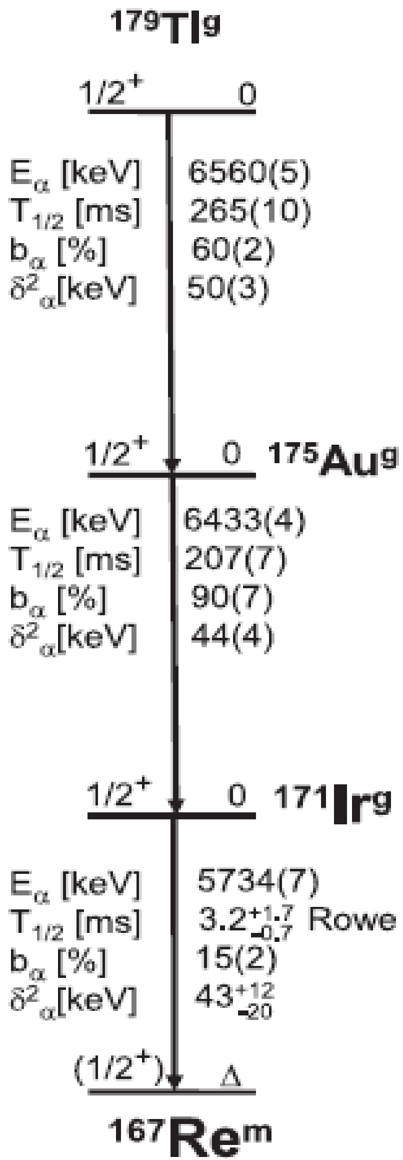

Unhindered α decays point to the pure $s_{1/2}$ configuration in all these nuclei.

The measurement of μ(^{175}Au) is needed to confirm this interpretation

Large hindrance of α decay $^{180}Tl^{g} \rightarrow ^{176}Au^{g}$

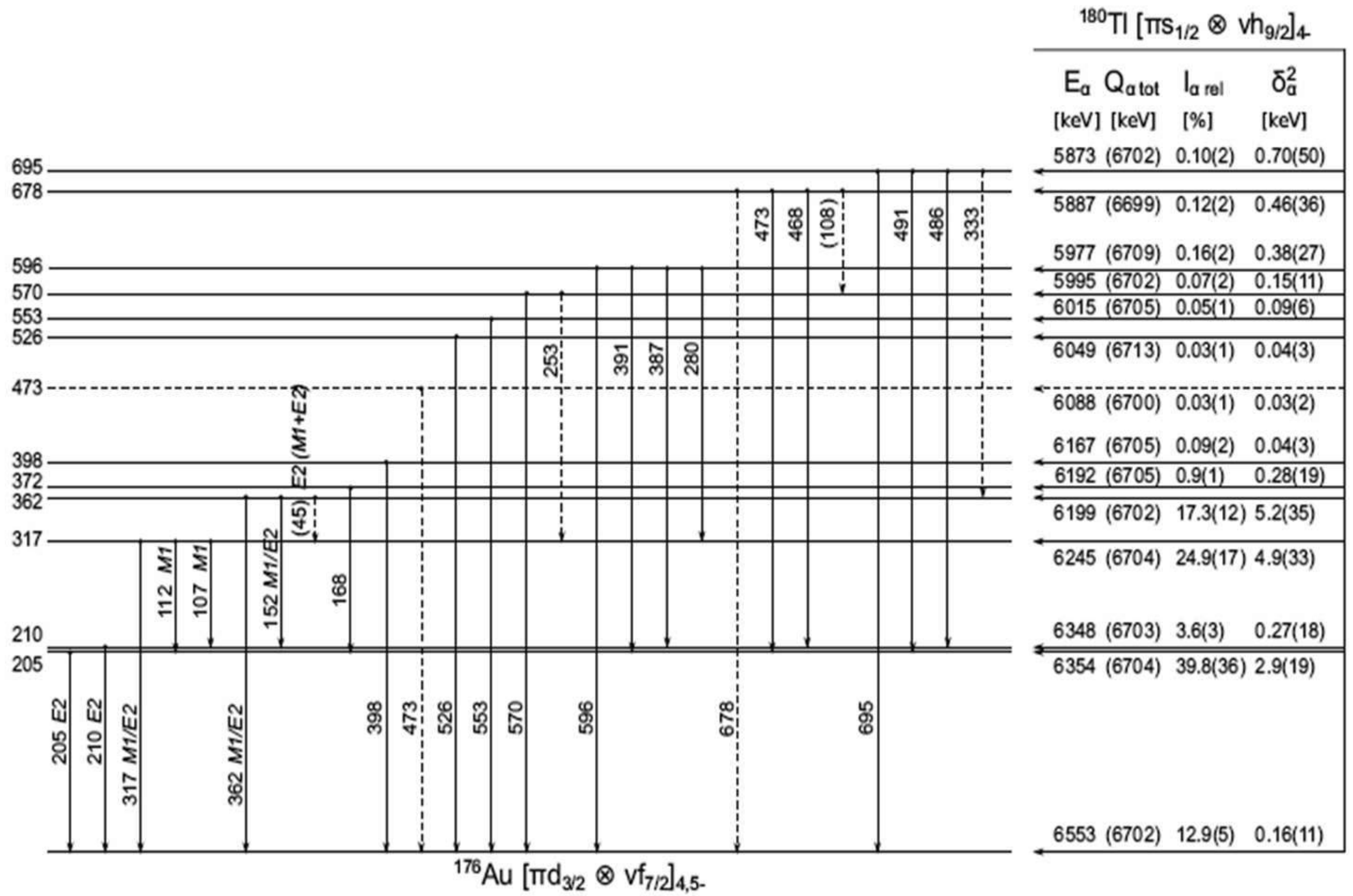

Large hindrance of α decay $^{180}Tl^{g} \rightarrow ^{176}Au^{g}$

^{178}Tl		^{180}Tl		^{182}Tl		^{184}Tl	
E_α(keV)	δ^2(keV)	E_α(keV)	δ^2 (keV)	E_α(keV)	δ^2 (keV)	E_α(keV)	δ^2(keV)
6862(10)	**0.30(15)**	**6553(7)**	**0.16(11)**	6406	0.043(25)	6161	0.57(6)
6693(10)	13.0(17)	6354(7)	2.9(19)	6360(6)	0.048(28)	5988(12)	2.4(4)
6595(10)	10.2(24)	6348(7)	0.27(18)	6165(6)	1.13(66)	5964(12)	
		6245(7)	4.9(33)	6046(5)	5.8(34)	5810(12)	0.9(1)
		6199(7)	5.2(35)	5962(5)	6.0(35)	5748(12)	< 0.09

Strongly hindered gs→gs decay ($\delta^2 \sim 0.1$keV; HF~500) at the same spin and deformation! Large hindrance is due to the change of both proton, $s_{1/2} \rightarrow d_{3/2}$, and neutron, $h_{9/2} \rightarrow f_{7/2}$, configurations (confirmed by μ measurements).

Why does neutron in ^{176}Au occupy $f_{7/2}$ instead of expected $h_{9/2}$ orbital?

Nuclear shells below N = 100

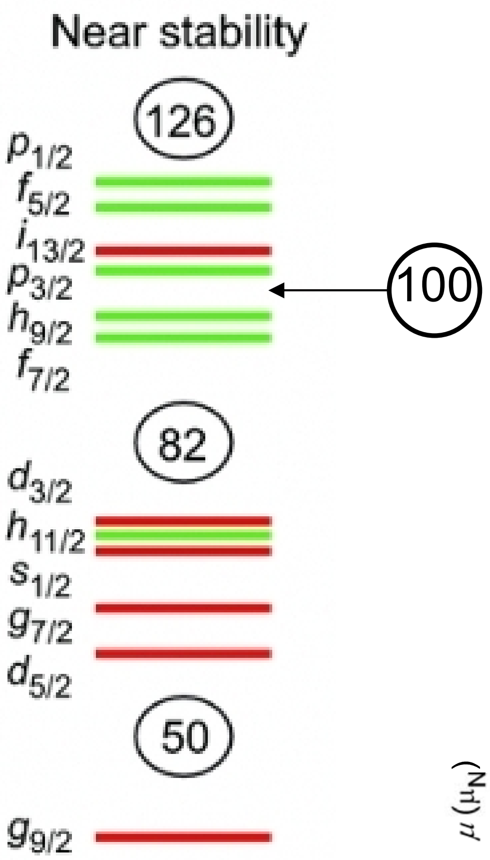

All N = 83 (85) nuclei are of $\nu f_{7/2}$ configuration: spin, parity, μ (from ${}_{54}Xe_{83}$ to ${}_{70}Yb_{83}$)

N = 99: ${}^{181}Pb_{99}$, 9/2—, $\nu h_{9/2}$

${}^{179,177}Hg_{99,97}$, 7/2— and μ coincides with μ(N = 83)

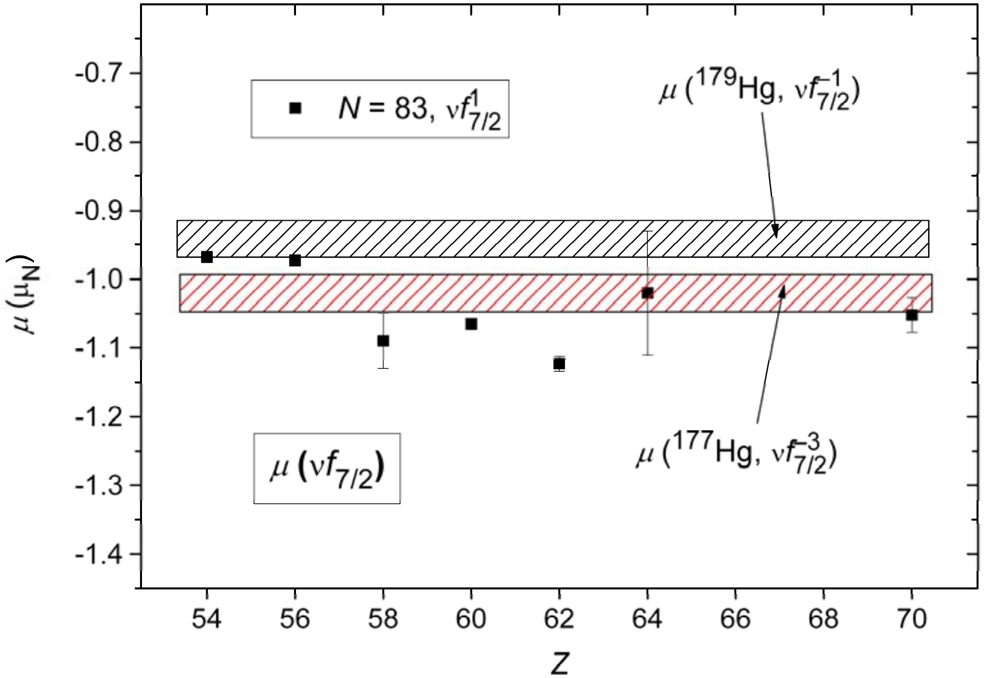

Nuclear shells below N = 100

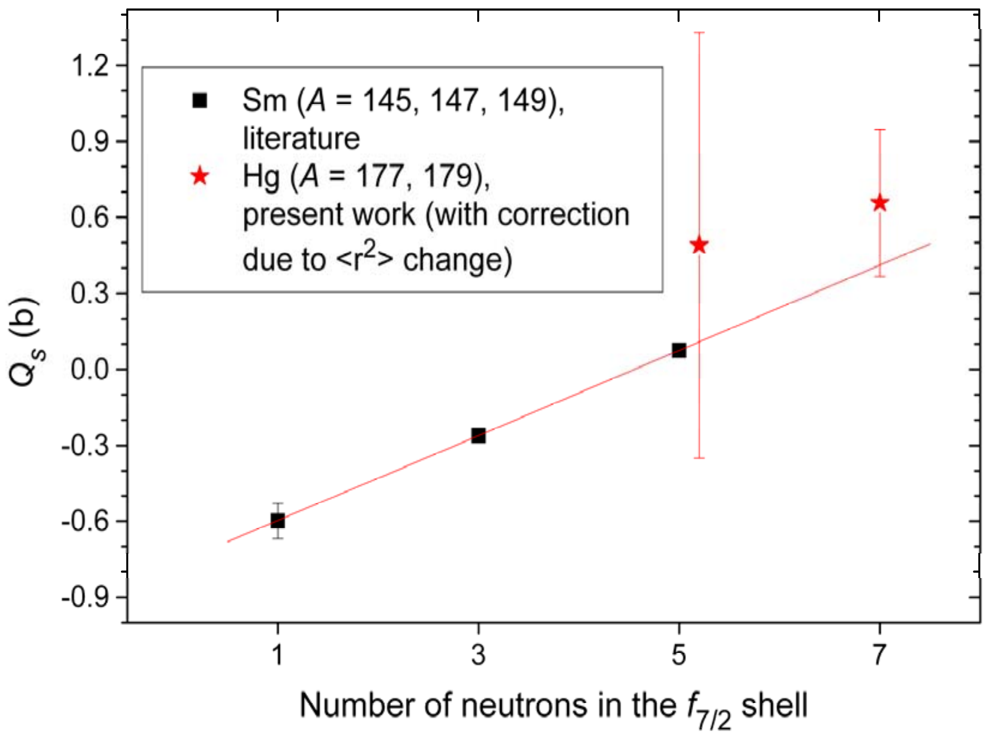

Pure shell model — seniority scheme for the filling *j*-shell (*n* is a number of neutrons): linear dependence of Q_S on *n*

Exp. data for *Q* confirm the pure shell-model $f_{7/2}$ configuration for $^{177,179}Hg_{97,99}$

$$\left\langle j^n \mid \hat{Q} \mid j^n \right\rangle = \frac{2j+1-2n}{2j+1-2\nu} \left\langle j^\nu \mid \hat{Q} \mid j^\nu \right\rangle = \frac{5}{3} Q_{s.p.}(\nu f_{7/2}) - \frac{1}{3} Q_{s.p.}(\nu f_{7/2}) \cdot n$$

Shell evolution

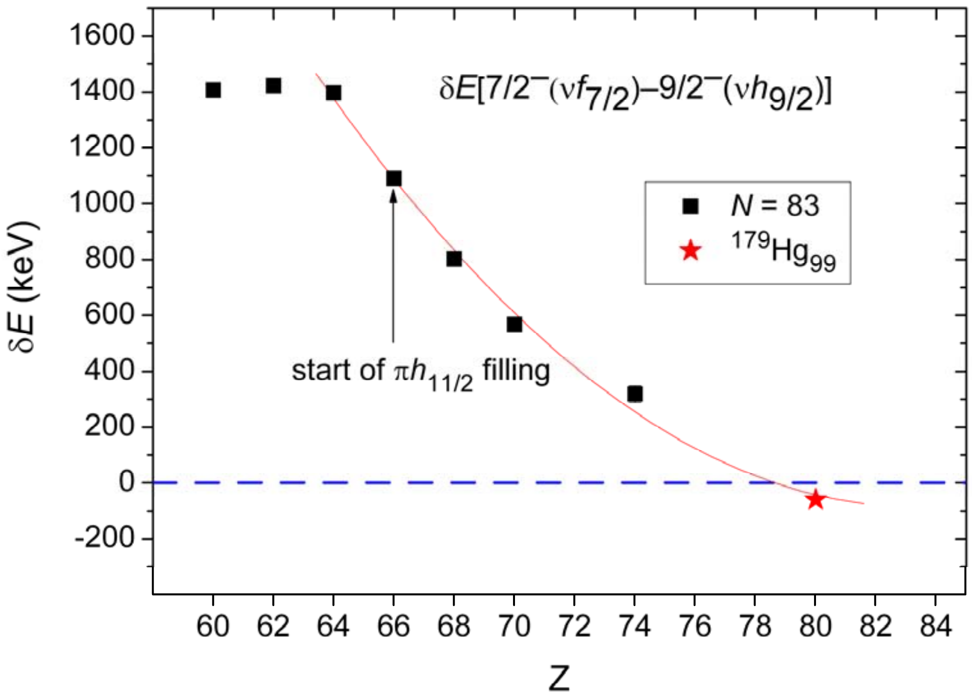

$^{160}Re_{85}$: Changing single-particle structure beyond the proton drip line

The convergence of the $h_{9/2}$ and $f_{7/2}$ neutron levels could open up a γ -decay path from the high-spin isomer to the low-spin ground state of ^{160}Re, providing a natural explanation for the anomalous absence of charged-particle emission.

I.G. Darby et al. Phys. Lett. B 695 (2011) 78

One expects the proton–neutron tensor force component acting between protons filling the $1h_{11/2}$ orbital and a single neutron in the $1h_{9/2}$ or $2f_{7/2}$ orbitals to modify their relative single-particle energies

L. Bianco et al. / Physics Letters B 690 (2010) 15

Shell swap

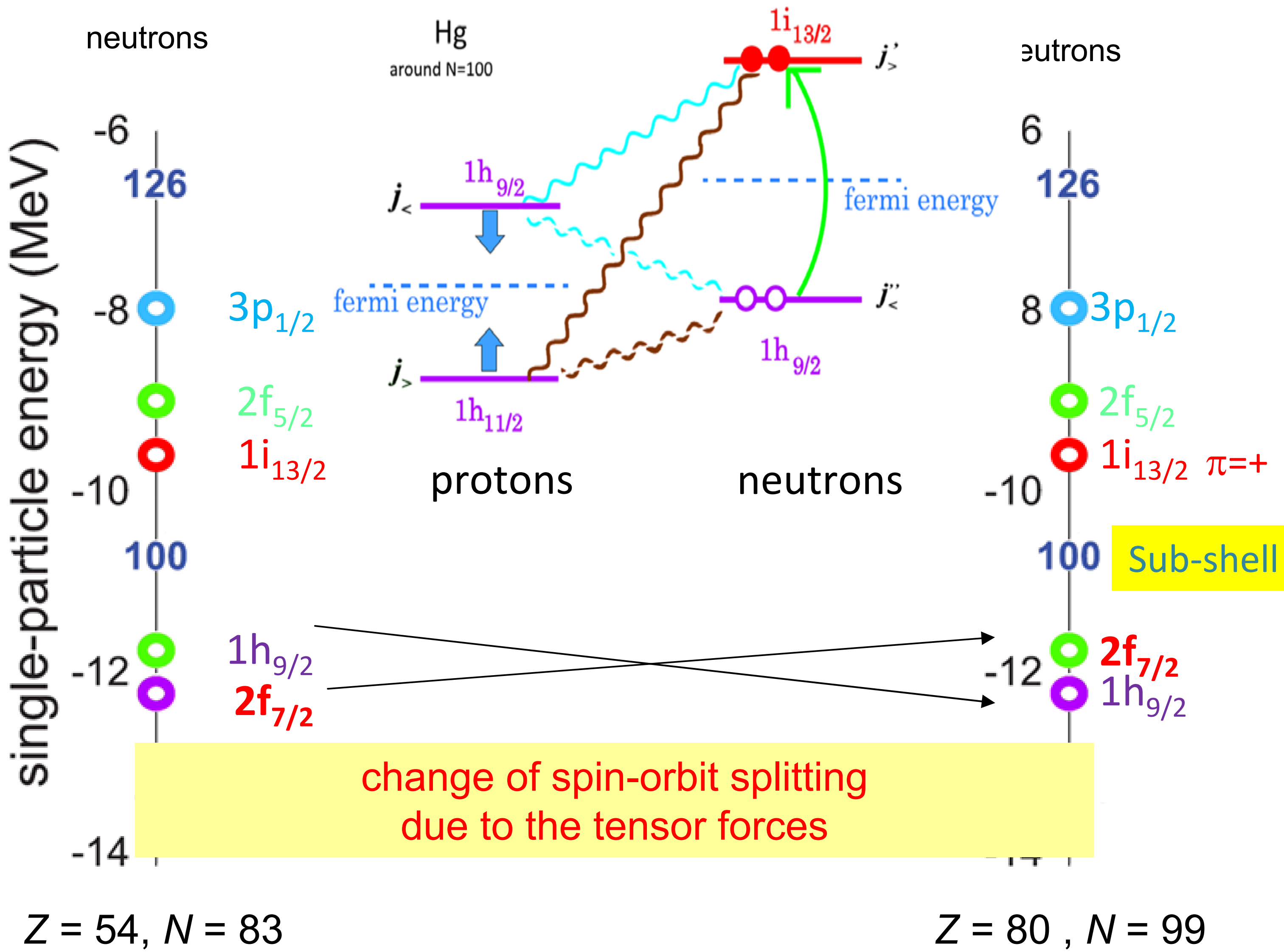

T Otsuka and Y Tsunoda J. Phys. G: 43 (2016) 024009

Shell swap

Au

Configuration	I	$\mu_{add}(\mu_N)$	$\mu_{exp}(\mu_N)$
$\boldsymbol{\pi d_{3/2} \otimes \nu h_{9/2}}$	**4**	**–0.84**	**–0.834(9)**
$\pi d_{3/2} \otimes h_{9/2}$	4	0.66	-0.834(9)

Tl

Configuration	I	$\mu_{add}(\mu_N)$	$\mu_{exp}(\mu_N)$
$\boldsymbol{\pi s_{1/2} \otimes \nu h_{9/2}}$	**4**	**–0.58**	**–0.564(23)**
$\pi s_{1/2} \otimes \nu f_{7/2}$	4	0.70	–0.564(23)

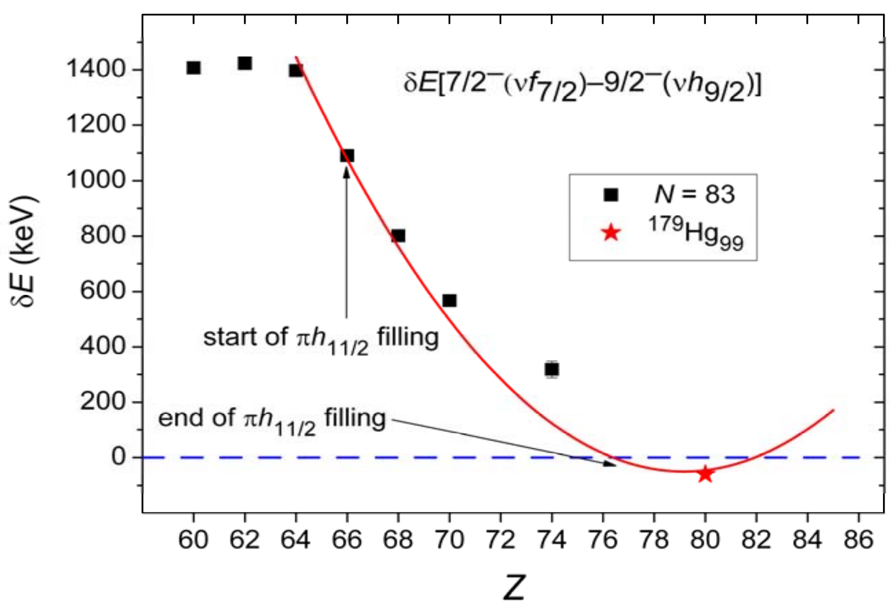

$\mu(^{176}Au_{97})$ is explained only with $\nu f_{7/2}$ assumption for neutron configuration (additivity relation)

$\mu(^{180}Tl_{99})$ is explained only with $\nu h_{9/2}$ assumption for neutron configuration

$^{181}Pb_{99}$ — $\nu h_{9/2}$ configuration:
$I\ (^{181}Pb_{99}) = 9/2$

Subshells return to the "normal" ordering at Z > 80

Shape Coexistence in the Pb region

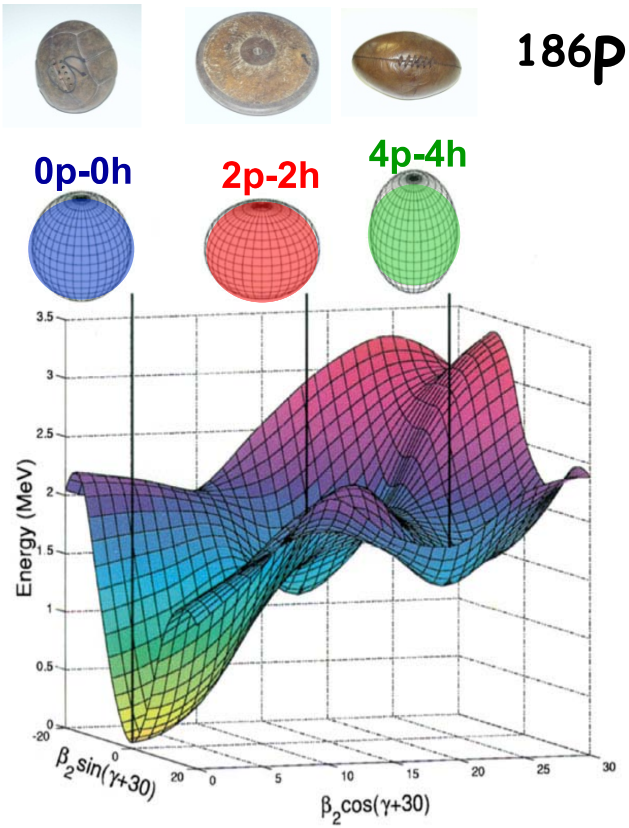

^{186}Pb

Potential Energy Surface for ^{186}Pb

A.Andreyev et al. Nature, 405, 430 (2000)

•Pb (Z=82) g.s.: p(0p-0h) – spherical

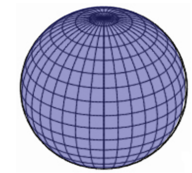

Proton pair excitations across Z=82 shell gap (neutrons are spectators):

•1 pair excitation: p(2p-2h) -oblate

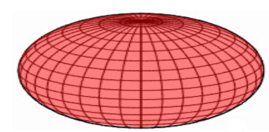

•2 pair excitation: p(4p-4h) -prolate

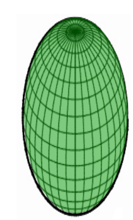

K. Heyde et al., Phys. Rep. 102 (1983) 291
J.L. Wood et al., Phys. Rep. 215 (1992) 101
A. Andreyev et al., Nature 405 (2000) 430
K. Heyde and J. Wood, Rev. Mod. Phys., 83, 1467 (2011)

Mercury Chain (Z=80)

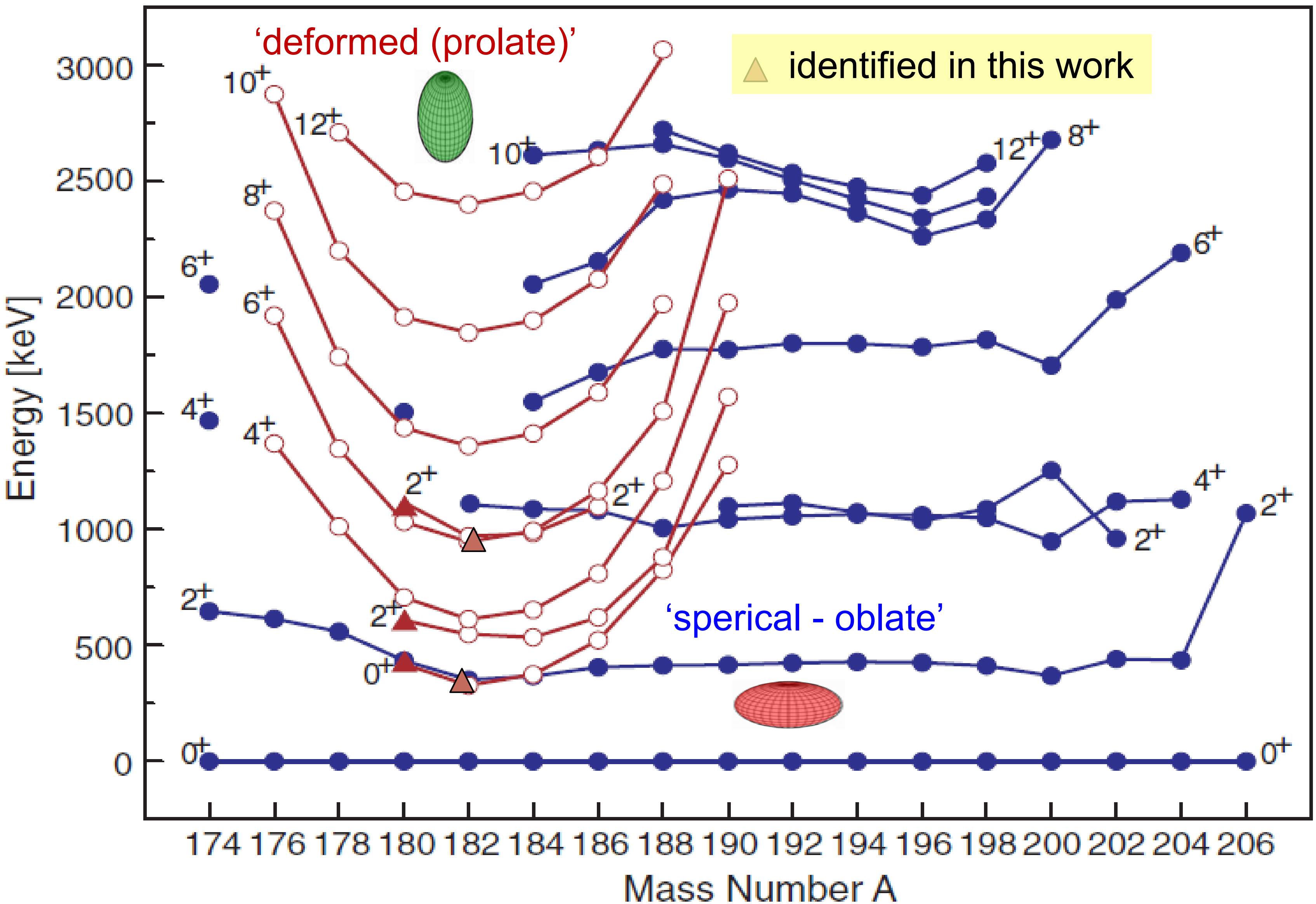

Intruder states

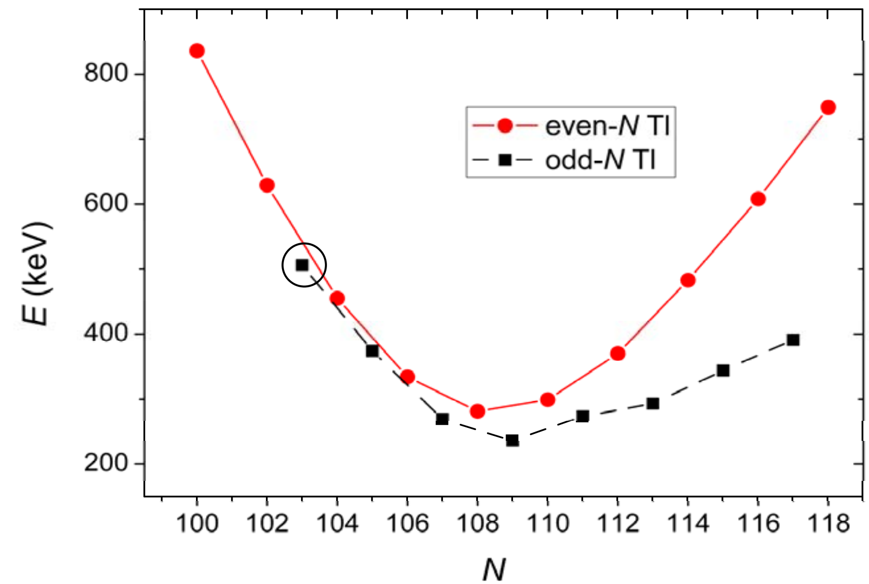

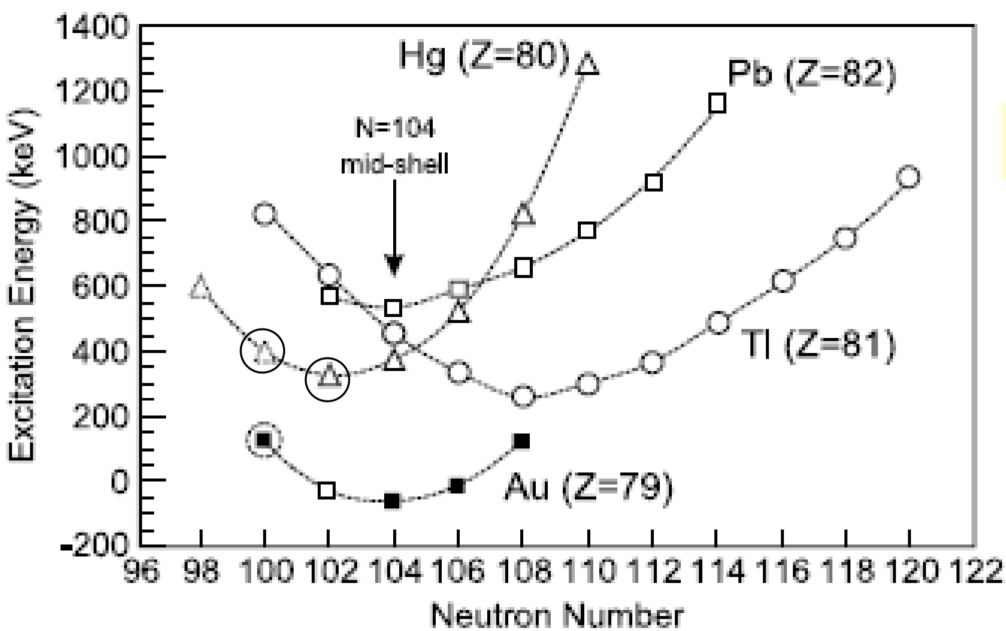

◯ identified in this work

Intruder states

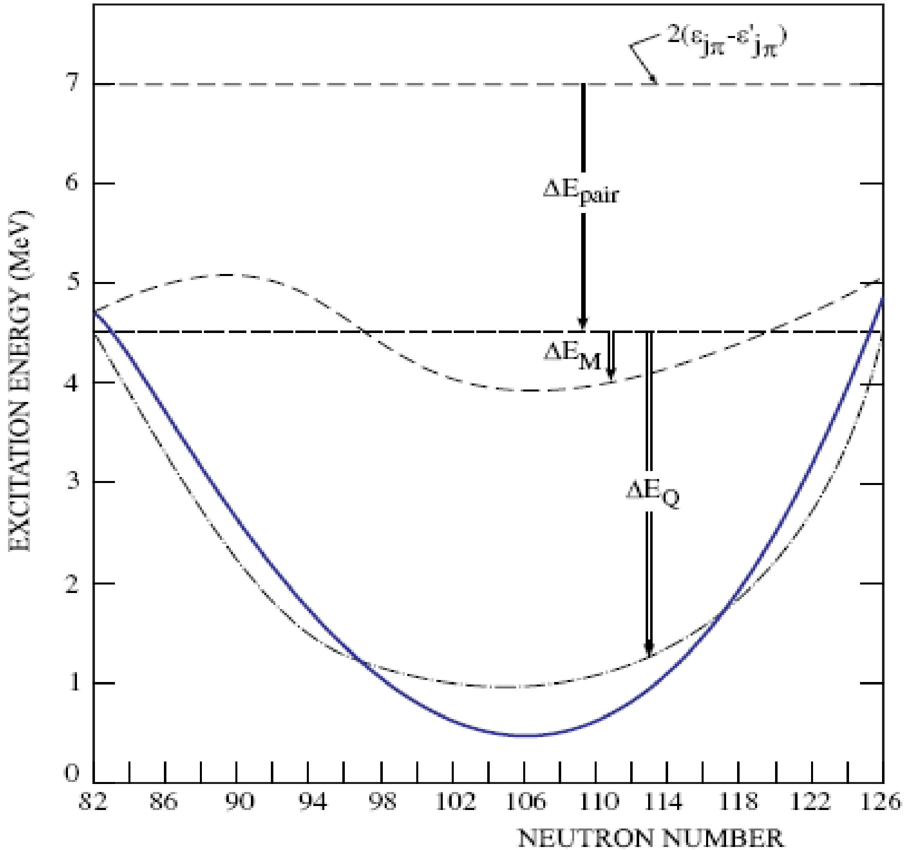

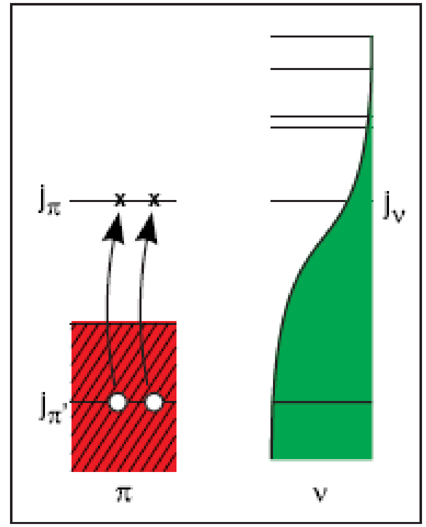

$$\Delta E_Q = k \cdot n_{\nu,val} \cdot (\Omega - n_{\nu,val}) \cdot n_{p-h}$$

$n_{\nu,val}$ – number of valence neutrons

Ω – degeneracy of the neutron shell

The different energy terms, contributing to the energy of the lowest proton 2p-2h 0^+ intruder state for heavy nuclei. The unperturbed energy, the pairing energy, the monopole energy shift, and the quadrupole energy gain are presented,

K. Heyde and J.L. Wood, Rev. Mod. Phys. 83, 1467 (2011)

Intruder states

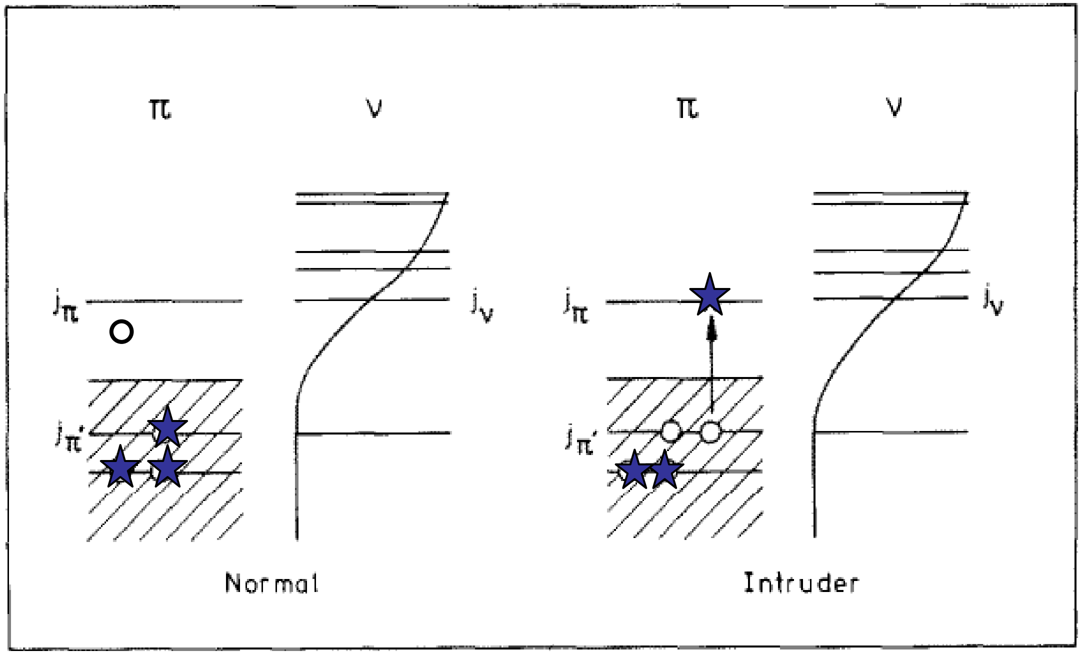

Schematic representation of a proton 1p2h intruder configuration (Tl)

Mixing of configurations with different shapes

$\alpha_C(2_2^+ \rightarrow 2_1^+)$:

^{180}Hg	3.5(4)	
^{182}Hg	7.2(13)	[cf. α_C(M1) = 1.15; α_C(E2) = 0.42]
^{184}Hg	14.2(3.6)	

} E0 transition exists

$$\rho^2(E0) = \frac{Z^2}{R_0^2} a^2 (1 - a^2) \left[\delta \left\langle r^2 \right\rangle \right]^2$$

The large conversion coefficient for the 2_2^+ to 2_1^+ transition in ^{182,184}Hg is a strong fingerprint of shape coexistence as strong E0 transitions are the result of considerable mixing of two states with a large difference in deformation. Combining the measured conversion coefficients with the re-evaluated B(E2) values from the Coulomb excitation experiments will result in E0 transition strength ρ^2(E0) values which can be compared with different theoretical models

Conclusions

Изомерно селективная фотоионизация в лазерном ионном источнике позволяет получить большой объем ядерно-спектроскопической информации ($T_{1/2}$, E_{α}, b_{α}, b_{β}, α-γ, γ -γ coincidence, conversion coefficients, partial decay schemes и т. д.) без дополнительных затрат времени.

Из полученных результатов отметим:

1. Сопоставление фактора задержки α распада $^{181}Tl \rightarrow ^{177}Au$ со спинами и магнитными моментами этих ядер позволяет сделать вывод о неаксиальной деформации ^{177}Au;
2. Большой фактор задержки α распада $^{180}Tl \rightarrow ^{176}Au$, а также анализ спинов и моментов соседних изотопов Hg указывает на изменение оболочечной структуры (shell swap).
3. Обнаружен новый интрудер изомер в ^{184}Tl, подтверждена параболическая зависимость энергии возбуждения этих изомеров от числа нейтронов.
4. Аномально большие коэффициенты конверсии для $2_2^+ \rightarrow 2_1^+$ переходов в $^{180,182,184}Hg$ свидетельствуют о сильном смешивании состояний с разной деформацией.